Article

Investigation of the Influence of PLA Molecular and Supramolecular Structure on the Kinetics of Thermal-Supported Hydrolytic Degradation of Wet Spinning Fibres

Malgorzata Gieldowska [1], Michal Puchalski [1,*], Grzegorz Szparaga [1], Izabella Krucinska [1]

[1] Lodz University of Technology, Institute of Material Science of Textiles and Polymer Composites, Centre of Advanced Technologies of Human-Friendly Textiles 'Pro Humano tex';
malgorzata.gieldowska@dokt.p.lodz.pl (M.G.); grzegorz.szparaga@p.lodz.pl (G. S.);
izabella.krucinska@p.lodz.pl (I. K.)

* Correspondence: michal.puchalski@p.lodz.pl (M.P.); Tel.: +48 42 631 33 22

Abstract: In this study, differences in the kinetics of thermal-supported hydrolytic degradation of poly(lactic acid) (PLA) sample wet spinning fibres due to material variance in the initial molecular and supramolecular structure were analysed. The investigation was carried out at the microstructural and molecular levels by using readily available methods such as scanning electron microscopy, mass erosion measurement and estimation of intrinsic viscosity. The results show a varying degree of influence of the initial structure on the degradation rate of studied PLA fibres. The experiment shows that hydrolytic degradation at a temperature close to the cold crystallization temperature on a macroscopic level is definitely more rapid for the amorphous material, while on a molecular scale it is similar to a semi-crystalline material. Further, for the adopted degradation temperature of 90 °C, a marginal influence of pH of the degradation medium on the degradation kinetics was also demonstrated.

Keywords: polylactide; thermal degradation; hydrolytic degradation; fibres; kinetic of erosion; kinetics of degradation

1. Introduction

Poly(lactic acid) or polylactide (PLA) is the most commonly used biodegradable material, produced from completely renewable sources such as sugar, corn or other vegetables [1]. This thermoplastic aliphatic polyester exhibits similar mechanical properties as popular petroleum-based polyesters, with additional special properties such as compostability and biocompatibility/bioresorbability [2,3]. According to the physical and chemical properties, PLA is a promising alternative to petroleum-based polymers from the application point of view. PLA can be used to form foams [4,5], films [6], fibres [7–9] and nonwovens [10,11] designed for many different applications, from medical [12,13] to agricultural [14,15] use.

Commercially available PLA is synthesised by polycondensation of lactic acid (poly(lactic acid)) or ring-opening polymerisation of lactide obtained from the depolymerisation of oligomers of lactic acid (polylactide), which is a product of the fermentation of biomass, such as corn [16].

The physical and chemical properties of final PLA products depend on chilarity of the polymer chain, and from different supramolecular structures of polymer chains. The high chirality of PLA chains reduces its ability to create a crystalline phase, which has a strong influence on the useful properties of final products [17,18].

Peer-reviewed version available at Materials 2020, 13, 2111; doi:10.3390/ma13092111

PLA is also well known as a hydrolysable and unstable biodegradable polyester. Degradation of this aliphatic polyester depends on the physical, chemical and biological agents used and is an interesting subject from the scientific point of view. The degree and rate of degradation also depend on the molecular and supramolecular structures of the polymer. The current state of knowledge on PLA is based on experiments carried out under laboratory and natural conditions. The described results of analysing degradation under laboratory conditions are focused on the influence of the content of D-lactide isomer [19], the crystalline form [20], the content of nanomaterials [21,22] and the pH and temperature of the degradation medium [23] on the rate of hydrolytic degradation, which is the main way of PLA degradation; however, the tests were carried out on model samples and applied a limited number of degradation factors. The results presented in these works testify that hydrolytic degradation of polymer structures lasts up to many weeks and it is favourable to conduct it in conditions close to the glass transition temperature of the polymer [24–26]. Other investigations of PLA degradation carried out under laboratory conditions are thermal degradation [27,28], artificial weathering [29,30] and composting [31,32].

An interesting issue in the field of life cycle assessment of PLA materials is testing in real conditions, in which the true degradation time of PLA products can be verified. These tests should take into account climatic conditions and the environment, including soil composition, and degradation time may be even several years depending on the structure of the initial material [33,34].

In this paper, the results of investigating the influence of the initial molecular and supramolecular structure of polylactide on the thermal-supported hydrolytic degradation of PLA wet-spinning fibres are presented. The experiment was carried out with fibres characterized by various molecular structures, including molar mass and content of D-lactide isomer of the polymer, and various supramolecular structures, especially degree of crystallization and crystal form. The process of degradation was carried out in a selected water base medium with pH 3.5, 5 and 10, under temperatures near the cold crystallization point, 90 °C. The reason to conduct the process of degradation at an elevated temperature was to reduce the time of the experiment and also to check how the temperature-induced thermal condition inducing crystallization of PLA affected the rate of hydrolytic degradation [35]. The detailed information about the fibres, their properties and the methodology of how they were made were presented earlier [36]. The performed experiment allows us to clarify how the initial molecular and supramolecular structure of PLA impacts the rate of thermal-supported hydrolytic degradation of real objects that are ready for practical application such as wet-spinning fibres. The degradation progress was measured as mass loss, supplemented by photographic and scanning electron microscopy (SEM) documentation, and analysis of the change in intrinsic viscosity as the parameter characterising the degradation on the molecular level. The obtained results were numerically analysed in order to determine the factors of kinetic degradation at the molecular and macroscopic levels, which is important data in the evaluation of the influence of the structure of the initial material on the rate of degradation in the example of real objects such as fibres.

2. Materials and Methods

2.1. Materials

An investigation of the influence of initial molecular and supramolecular structures of PLA on the rate of thermal-supported hydrolytic degradation was performed on wet spinning fibres made from a commercially available polymer, PLA Ingeo (Nature Works LLC, USA), as described in detail by Puchalski et al. 2018 [36]. Table 1 shows the main parameters of the applied polymer, including NatureWorks symbol, content of D-lactide isomer, weight-average molar mass (M_w), dispersity (M_w/M_n) and the structural parameters of the studied samples: total draw ratio during fibre processing, crystal form, degree of crystallinity (χ_c) and linear mass.

Table 1. Main characteristics of studied fibres and raw materials.

Sample	Characteristic of Raw Polymer				Characteristic of Fibre			
	NatureWorks symbol of PLA	Contents of D-lactde isomer (%)	M_w (kg/mol)	M_w/M_n	Total Draw Ratio (%)	Crystal form*	χ_c** (%)	Linear mass
PLA12-DR400	Ingeo 4060D	12	119	1.40	400	-	amorphous	158.00 (2.09***)
PLA12-DR600	Ingeo 4060D	12	119	1.40	600	α'	1.2	80.33 (0.90)
PLA2.5-DR450	Ingeo 2002D	2.5	112.6	1.46	450	α'	16.6	121.00 (1.43)
PLA2.5-DR550	Ingeo 2002D	2.5	112.6	1.46	550	α'	33.5	72.67 (0.79)
PLA1.4-DR500	Ingeo 6201D	1.4	59.1	1.29	500	α'	47.6	96.00 (1.04)
PLA1.4-DR650	Ingeo 6201D	1.4	59.1	1.29	650	α	53.8	68.33 (0.52)

*Parameter determined by using WAXD method.
**Value estimated by using DSC method.
*** Coefficient of variation is in brackets.

2.2. Methodology of thermal-supported hydrolytic degradation

The hydrolytic degradation process was carried out in 3 selected mediums based on distilled water with various pH: pH 10 (water solution of sodium carbonate), pH 5 and pH 3.5 (water solution of acetic acid). Samples of the same mass, 5 g, were degraded in 50 mL of hydrolytic medium under a controlled temperature of 90 °C for 1, 2, 3, 4, 5, 6, 7, 10, 14 and 21 days.

2.3. SEM method

The effects of degradation on the change of PLA fibre morphology were studied by using photography documentation and a NovaNanoSEM 230 scanning electron microscope (SEM) from FEI Company (Netherlands). For SEM measurement, the fibre samples were prepared by fixing the parts of fibres to an SEM holder using conducting carbon adhesive tape. The studies were carried out using low-vacuum mode and beam energy of 10 keV, which eliminated the requirement to cover the sample with a conductive material such as gold.

2.4. Mass loss

The measurement of mass after degradation of samples, which were cleaned with distilled water, was conducted using a PS.R1 precision balance (Radwag, Poland). The mass percent remaining after time of degradation (D_t) was calculated according to the following equation:

$$D_t = \frac{m_t}{m_0} 100\% \quad (1)$$

where m_0 and m_t are the masses of the sample before and after degradation, respectively.

2.5. Intrinsic viscosity

Structural changes at the molecular level during thermal-supported hydrolytic degradation were estimated by determining the intrinsic viscosity of diluted polymer/dichloromethane (0.08 g/dL) using an Ubbelohde viscometer (Type 2a, Poland) at 25 °C. The relationship between

viscosity-average molecular weight (Mη) and estimated intrinsic viscosity [η] can be described by the following Mark–Houwink equation [37]:

$$[\eta] = KM_{\eta}^{\alpha} \quad (2)$$

where K and α are constants, which for PLLA equal 1.124×10^{-2} and 0.52, respectively, and satisfactorily describe the tested PLA from Nature Works LLC with a slight content of D-lactide isomer [38]. Since the studied polymers changed at the molecular level during degradation, an analysis of estimated intrinsic viscosity change as a function of degradation time was performed.

3. Results and Discussion

3.1. Photographic documentation and SEM results

First, the changes of morphology of the PLA fibres after the thermal-supported hydrolytic degradation process were characterized. All of the investigated samples were completely degraded after 21 days. Figure 1 shows selected photographs of the degradation process of the studied samples occurring in various hydrolysed mediums. According to these photographs, the physical changes of samples during thermal-supported hydrolytic degradation depended on the initial ordering and crystallinity of the sample, and were visible as strong shrinkage after the first day of the experiment in the case of amorphous samples. The relationship between supramolecular ordering and the shrinkage phenomenon of the fibrous PLA structure was well known, as reported by, e.g., Puchalski et al. [39]. Shrinkage of fibrous materials resulted from the disordered pre-existing supramolecular structure of the polymer, which has a tendency towards relaxing and ordering, mainly during thermal processing. Therefore, the reason for their amorphous initial structure, the rapid and significant shrinkage of fibres obtained from PLA12, was possible to predict. The opposite occurred with fibres from PLA1.4, in which, due to the initial semicrystalline structure, the shrinkage was marginal. A very interesting phenomenon was observed in the investigation of thermal-supported degradation of fibres made from PLA2.5. The rapid shrinkage of fibres occurring with a lower draw ratio was observed, while in the case of fibres with a higher draw ratio, this phenomenon was insignificant. That result confirmed the relationship between shrinkage during thermal-supported hydrolytic degradation and the pre-existing supramolecular structure created in the technological regime. The next step of degradation was fragmentation, which was observed after the third and fifth days of degradation despite the ordering of the pre-existing supramolecular structure. According to the photographic documentation (Figures S1–S3), the most degradable fibres ware obtained from PLA with the highest D-lactide content and molar mass and amorphous supramolecular ordering; after the third day the samples were in powdered form, which was the effect of the first stage of the degradation process, fragmentation. During the degradation time, the volume of the samples decreased, suggesting significant mass loss, the kinetics of which are presented in the next part of this paper. The most important information obtained from the photographic documentation is the lack of a clearly visible influence of the change of pH of the hydrolytic medium on the rate of degradation. Regarding the organoleptic evaluation of the degradation effects, it can only be concluded that in the case of thermal-supported hydrolytic degradation, the initial structure of the polymer and the regimes of its processing, which determine the ordering and crystallinity of the fibres, have a significant influence on the rate of degradation.

Peer-reviewed version available at Materials 2020, 13, 2111; doi:10.3390/ma13092111

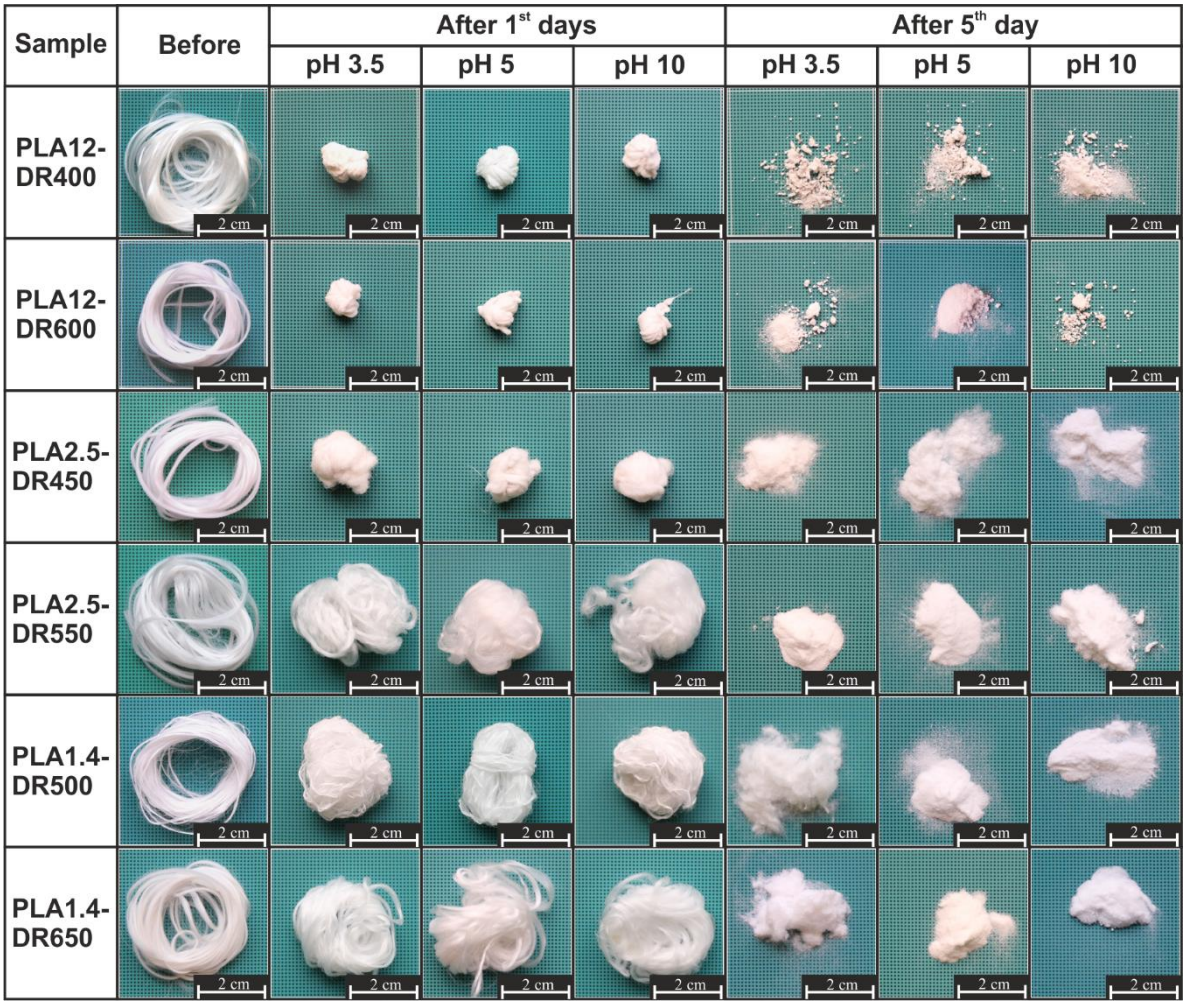

Figure 1. Photographic documentation of thermal-supported hydrolytic degradation of fibres obtained from PLA.

A more exhaustive analysis of the morphological structure changes of PLA fibres during degradation was obtained by using scanning electron microscopy. Figure 2 shows representative SEM images of samples before and after 7 days of thermal-supported hydrolytic degradation recorded at a magnification of ×2000. The initial structures of investigated samples were different. The PLA12-DR400 and PLA12-DR600 fibres were characterised by the least textured surface, the surface of PLA2.5-DR450 and PLA2.5-DR550 fibres was wavy, while the surface texture of PLA1.4-DR500 and PLA1.4-DR650 was smooth but contained transverse elements occurring periodically. The SEM results after 7 days of degradation clearly showed the evolution of morphology of samples as the result of various mechanisms of thermal-supported degradation. All studied materials were fragmented after 7 days, which is the first stage of degradation of polymeric materials. The degradation of the studied materials was combined with the process of PLA disintegration and fragmentation, which takes place in the areas of erosion of amorphous structure of the fibre material, which was described in detail by Azimi et al. [40]. This was confirmed by the presence of transverse cracks in the samples, especially in PLA12-DR400 and PLA12-DR600. The last degradation mechanism that was clearly visible was erosion, mainly surface erosion, as illustrated by the changes of surface texture of the studied samples. The analysis of the investigations by SEM showed differences in the degradation rate of studied samples, varying by initial polymer structure and supramolecular structure of fibres. In the case of PLA12-DR400 and PLA12-DR600 samples, the amorphous SEM results are proof of rapid fragmentation before surface erosion. In contrast, the SEM results verify the strong tendency of surface erosion in semicrystalline samples PLA2.5-DR450 and PLA2.5-DR550, while the semicrystalline PLA1.4-DR500 and PLA1.4-DR650 samples underwent mainly fragmentation and erosion of the amorphous phase of materials.

Peer-reviewed version available at Materials 2020, 13, 2111; doi:10.3390/ma13092111

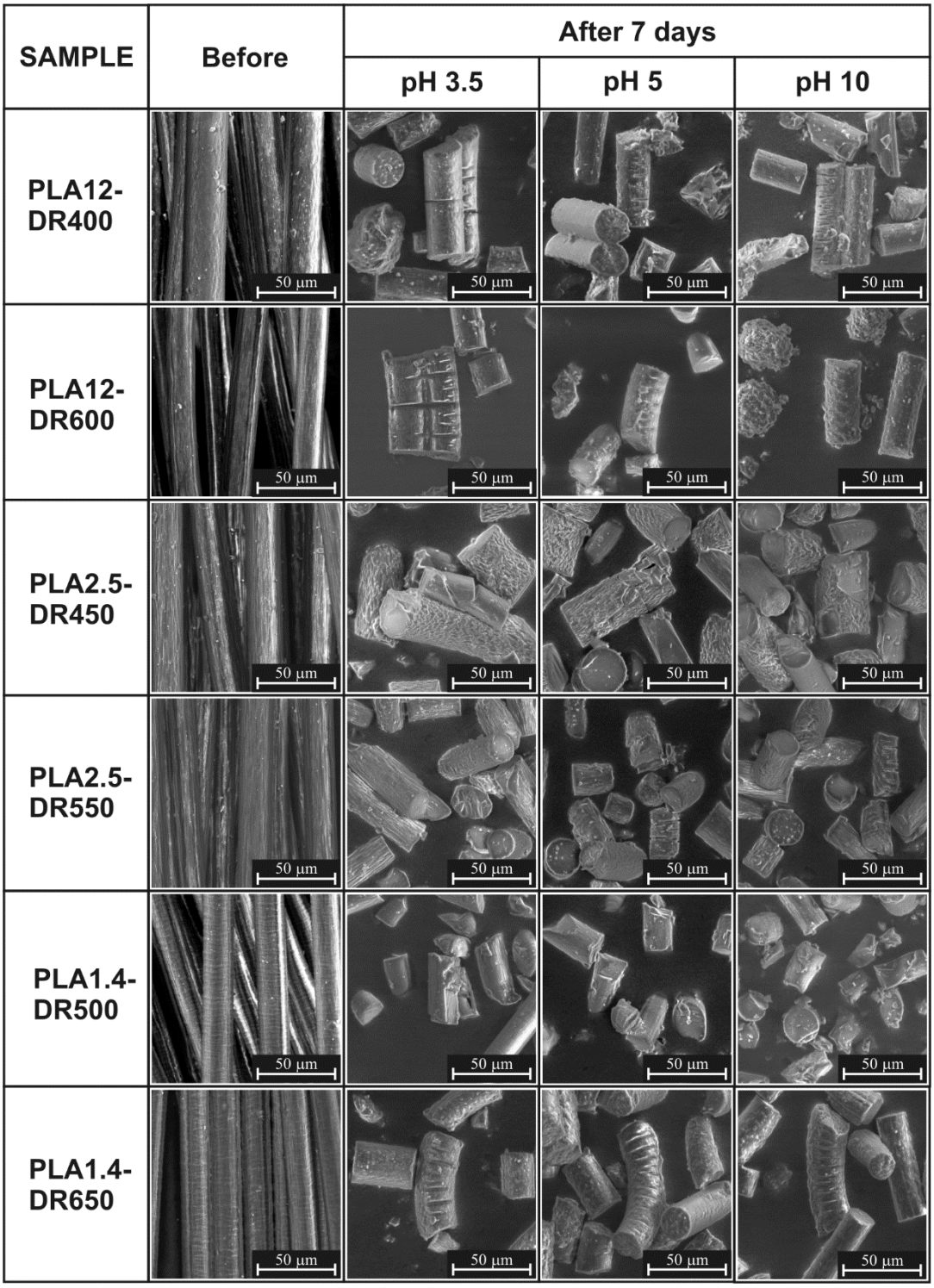

Figure 2. SEM results of studied samples recorded before and after 7 days of thermal-supported hydrolytic degradation.

3.2. Mass loss kinetics

The photographic documentation and SEM results clearly show the evolution of the samples' morphology during degradation at the macroscopic and microscopic scale, and verify the shrinkage, fragmentation and erosion of the studied fibrous materials. The next step of the investigation was to analyse mass loss in the function of degradation time measured as mass percent remaining, according to Equation (1). Figure 3 shows the changes of mass percent remaining (D_t) of studied samples during thermal-supported hydrolytic degradation in selected water solution with various pH levels. A significant increase of mass percent remaining for the samples obtained from PLA containing 2.5%

Peer-reviewed version available at Materials 2020, 13, 2111; doi:10.3390/ma13092111

and 12% D-lactide was observed after the second day, while for fibres obtained from PLA with 1.4% D-lactide it was only after the fifth day.

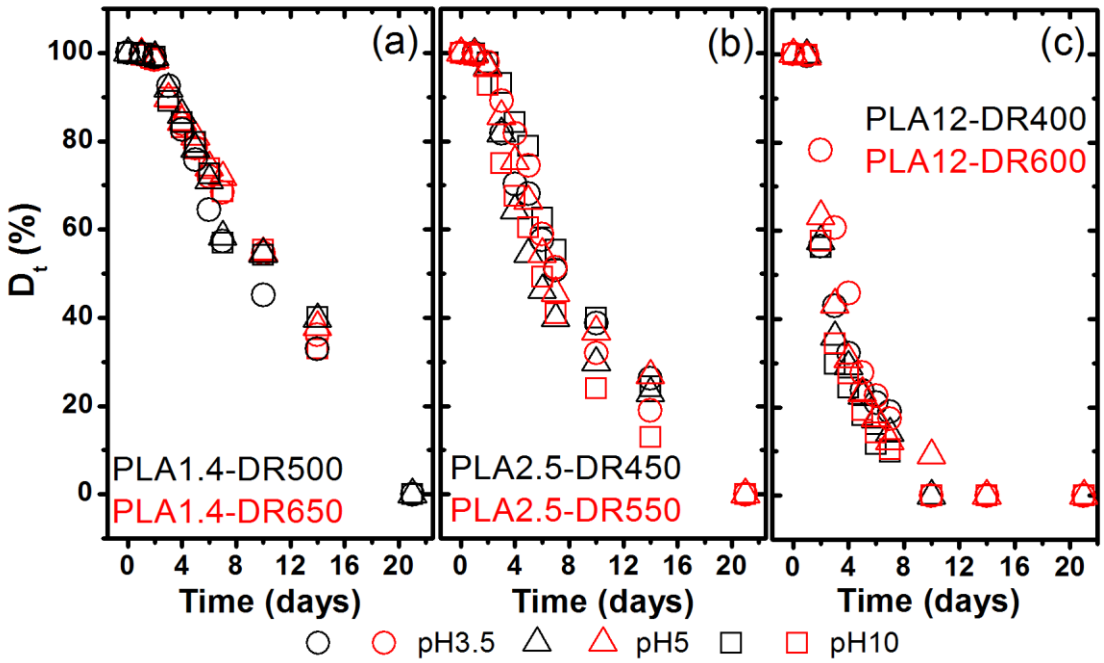

Figure 3. Changes of mass percent remaining of studied samples during thermal-supported hydrolytic degradation.

Table 1 shows estimations of the two characteristic kinetic parameters describing the typical erosion profile, onset time (t_{on}) and observed pseudo-first-order rate of erosion constant (k_e). The latter was characterized as a slope value according to the equation [41]

$$\ln(D_t) = A - k_e t \quad (3)$$

where D_t is mass percent remaining after time of degradation calculated according to Equation (1), t is the time of degradation starting from when erosion was significant, and A is an intercept. The calculated ton value is derived from intersecting the regression line in Equation (3) with the initial mass value as follows:

$$t_{on} = \frac{A - \ln(100)}{k_e} \quad (4)$$

Table 2. Kinetic parameters of mass percent remaining of studied samples during thermal-supported hydrolytic degradation.

SAMPLE	pH of medium	A±SE	k_e±SE (days^{-1})	R	t_{on} (days)
PLA12-DR400	pH 3.5	4.653±0.132	0.289±0.029	0.962	0.327
PLA12-DR400	pH 5	4.710±0.122	0.312±0.027	0.959	0.336
PLA12-DR400	pH 10	4.777±0.141	0.377±0.031	0.980	0.426
PLA12-DR600	pH 3.5	4.858±0.061	0.304±0.013	0.988	0.832
PLA12-DR600	pH 5	4.848±0.053	0.338±0.011	0.993	0.718
PLA12-DR600	pH 10	4.803±0.098	0.362±0.022	0.988	0.686
PLA2.5-DR450	pH 3.5	4.725±0.058	0.107±0.044	0.989	1.120
PLA2.5-DR450	pH 5	4.743±0.088	0.120±0.012	0.974	1.149
PLA2.5-DR450	pH 10	4.755±0.045	0.120±0.010	0.990	1.149
PLA2.5-DR550	pH 3.5	4.782±0.036	0.133±0.025	0.992	1.330
PLA2.5-DR550	pH 5	4.767±0.060	0.109±0.012	0.973	1.385

PLA2.5-DR550	pH 10	4.807±0.037	0.150±0.035	0.997	1.346
PLA1.4-DR500	pH 3.5	4.776±0.031	0.095±0.004	0.988	1.698
PLA1.4-DR500	pH 5	4.731±0.040	0.077±0.005	0.969	1.634
PLA1.4-DR500	pH 10	4.718±0.047	0.075±0.006	0.972	1.638
PLA1.4-DR650	pH 3.5	4.770±0.019	0.082±0.003	0.992	2.010
PLA1.4-DR650	pH 5	4.762±0.024	0.078±0.003	0.988	2.011
PLA1.4-DR650	pH 10	4.791±0.041	0.087±0.005	0.976	2.116

Considering the limited data points for each investigation, Table 1 shows good adherence to Equation (3) with a high correlation coefficient (R) and reasonably small relative standard error (SE) in k_e and intercept values estimated by the use of OriginPro 8.6 software. The analysis of estimated kinetic parameters of erosion profiles of PLA fibres degraded by thermal-supported hydrolysis clearly presents the influence of the initial PLA molecular structure on the pseudo-first-order rate constant and onset time values. The k_e increased with increased content of D-lactide isomer and decreased weight-average molar mass, as expected. It is worth noting that it is difficult to define the influence of the crystallinity degree of investigated samples on the pseudo-first-order rate of erosion constant value. In contrast, it is in the case of t_{on} where both the molecular structure of the initial polymer and the supramolecular structure of fibres influence this parameter. The onset time increased with increased content of D-lactide, weight-average molar mass and crystallinity degree. The highest pseudo-first-order rate of erosion constant, around 0.3 $days^{-1}$, and lowest onset time, around 0.35 days, characterized the amorphous PLA12-DR400 and PLA12-DR600 fibres, while for the PLA1.4-DR500 and PLA1.4-DR650 fibres, the maximum k_e was 0.095 $days^{-1}$ and 0.087 $days^{-1}$ and t_{on} was 1.698 days and 2.116 days, respectively. Thus, the experiment also showed that the pre-existing ordering and crystalline structure influenced the kinetics of PLA degradation in the proposed conditions, and the shortest onset time was observed for fibres characterized by amorphous structure (less than 1 day) and the longest onset time for materials with semicrystalline structure of ordered α form (more than 2 days).

3.2. Degradation kinetics of PLA fibres on molecular level

The degradation of polymers is mainly investigated on the molecular level by means of size exclusion chromatography (SEC) [42] or gel permeation chromatography (GPC) [43], by which it is possible to analyse the number average molar mass (M_n), weight-average molar mass (M_w) and dispersity (M_w/M_n). In our experiment, according to the possibilities of investigation, we decided to analyse the changes of fibres at the molecular level by means of a viscometer, which, according to Equation (2), allows that analysis to be performed.

The analysis of changes of measured intrinsic viscosity of PLA fibres during thermal-supported hydrolytic degradation was carried out up to the first 7 days, resulting from the strong mass loss after 7 days (described above) and finally in the impossibility of preparing experimental samples. Figure 3 shows the relative changes of [η] due to the medium with various pH levels. All studied samples indicated a change in molecular level after the first day, but the most intense was in the material formed from PLA containing 12% D-lactide isomer and characterized by the highest molar mass.

Preprints (www.preprints.org) | NOT PEER-REVIEWED | Posted: 16 April 2020 doi:10.20944/preprints202004.0255.v1

Peer-reviewed version available at Materials 2020, 13, 2111; doi:10.3390/ma13092111

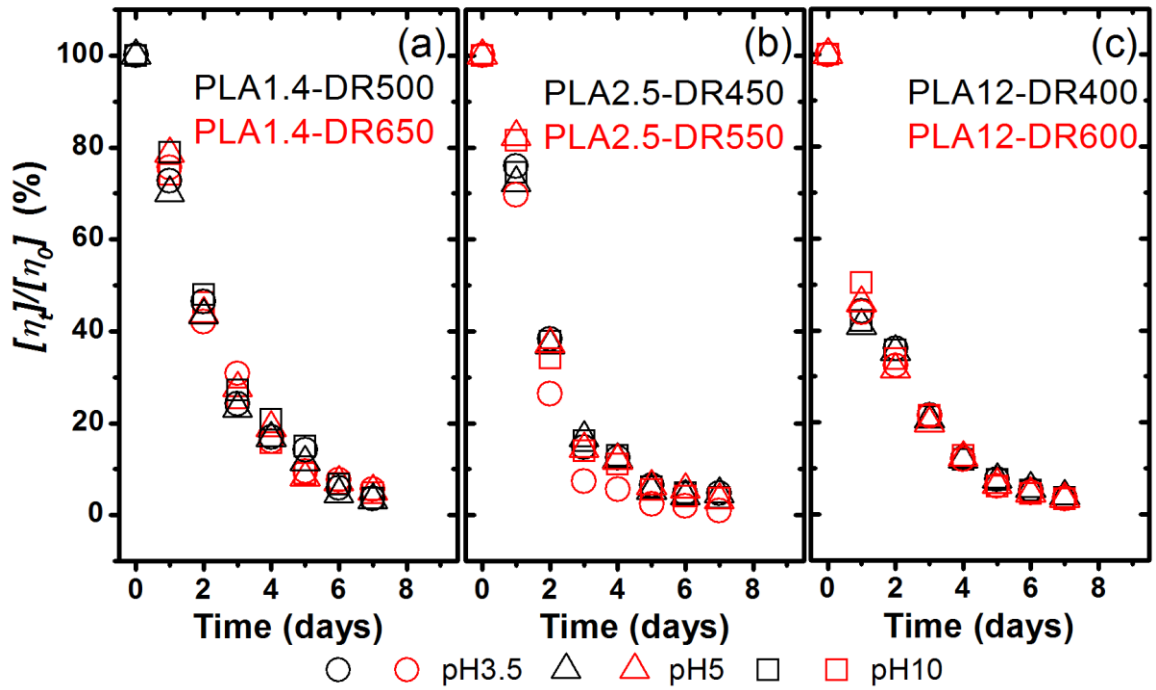

Figure 4. Changes of intrinsic viscosity percent remaining of studied samples during thermal-supported hydrolytic degradation.

To insightfully analyse the thermal-supported degradation rate of the studied samples, the degradation rate constant (k_d) was calculated from the decreased relative intrinsic viscosity based on the first-order kinetic model according to the following equation [44]:

$$\ln\left(\frac{[\eta_t]}{[\eta_0]}\right) = A - \alpha k_d t \quad (5)$$

where $[\eta_t]/[\eta_0]$ is the percentage change of intrinsic viscosity after time degradation $[\eta_t]$ due to initial intrinsic viscosity $[\eta_0]$, α is constant according to Equation (2), t is the time of degradation and A is an intercept.

According to the apparent degradation rate, the degradation time of half intrinsic viscosity is calculated by the following equation:

$$t_{50\%} = \frac{A - \ln(50)}{\alpha k_d} \quad (6)$$

The presented first-order kinetic model was used to describe the thermal-supported degradation of the studied fibres based on estimated intrinsic viscosity. Table 3 shows the kinetic parameters of the investigated degradation.

Table 3. Kinetic parameters of intrinsic viscosity percent remaining of studied samples during thermal-supported hydrolytic degradation.

SAMPLE	pH of medium	A±SE	k_d±SE (days^{-1})	R	$t_{50\%}$ (days)
PLA12-DR400	pH 3.5	4.599±0.160	0.686±0.039	0.970	1,09
PLA12-DR400	pH 5	4.572±0.179	0.702±0.044	0.962	1,09
PLA12-DR400	pH 10	4.593±0.168	0.704±0.040	0.959	1,19
PLA12-DR600	pH 3.5	4.437±0.094	0.651±0.023	0.985	1,35
PLA12-DR600	pH 5	4.438±0.079	0.654±0.019	0.989	1,29
PLA12-DR600	pH 10	4.503±0.084	0.670±0.020	0.988	1,31
PLA2.5-DR450	pH 3.5	4.568±0.186	0.659±0.044	0.954	1,15
PLA2.5-DR450	pH 5	4.557±0.190	0.676±0.045	0.954	1,06

Peer-reviewed version available at Materials 2020, 13, 2111; doi:10.3390/ma13092111

PLA2.5-DR450	pH 10	4.586±0.140	0.679±0.033	0.969	1,10
PLA2.5-DR550	pH 3.5	4.448±0.080	0.632±0.019	0.989	1,33
PLA2.5-DR550	pH 5	4.390±0.100	0.610±0.024	0.980	1,29
PLA2.5-DR550	pH 10	4.425±0.088	0.628±0.021	0.986	1,34
PLA1.4-DR500	pH 3.5	4.710±0.100	0.636±0.024	0.982	1,53
PLA1.4-DR500	pH 5	4.680±0.088	0.663±0.021	0.987	1,57
PLA1.4-DR500	pH 10	4.770±0.109	0.630±0.026	0.978	1,54
PLA1.4-DR650	pH 3.5	4.658±0.071	0.619±0.017	0.990	1,70
PLA1.4-DR650	pH 5	4.681±0.102	0.610±0.025	0.978	1,67
PLA1.4-DR650	pH 10	4.641±0.081	0.588±0.019	0.985	1,72

Similar to the mass loss kinetics analysis, Table 2 shows good adherence to Equation (5) with a high correlation coefficient (R) and relatively small relative standard error (SE) in k_d and intercept values estimated by OriginPro 8.6 to assess relative intrinsic viscosity change kinetics. However, the performed experiment clearly showed the various characteristics of degradation of the molecular structure of PLA more than the macroscopic mass erosion of the samples.

With regard to degradation at the molecular level, it is difficult to unequivocally find the influence of the initial polymer structure on the degradation kinetics. The estimated degradation rate values constantly decrease insignificantly with decreased content of D-lactide isomer and Mw and increased crystallinity degree. The influence of the initial structure on the kinetics of degradation is more pronounced for $t_{50\%}$ when it increases with the decreased content of D-lactide isomer and weight-average molar mass, and also with increased crystallization degree. It is worth noting that the degradation time of half intrinsic viscosity was less than 2 days for all studied samples and the highest was for the PLA1.4-DR650 sample, in which the crystalline α form was detected. The pH of the environment also has a slight influence on the kinetic factors of thermal-supported hydrolytic degradation of PLA fibers at the molecular level, but it is not possible to predict which pH value will be more favourable. For the most amorphous sample, the lower value of $t_{50\%}$ was estimated for pH 5, but for the most crystalline sample with α form crystal it was pH 3.5.

4. Conclusions

The main goal of this investigation was to present differences in the kinetics of hydrolytic degradation of PLA due to real material variance in the molecular and supramolecular structure of sample wet-spinning fibers. Complementary studies were realized on various levels by using selected methods such as SEM and viscosimetry.

The thermal-supported hydrolytic degradation experiment allows us to show the influences of temperature, or heat transfer, on the kinetics of hydrolytic degradation. In the sample erosion, decreasing molar mass (intrinsic viscosity) was significantly more rapid than at lower temperatures, the results of which are described in the cited literature.

From the macro- and microscopic point of view, all of the studied fibres became fragmented after just 3 days, and according to SEM results surface and volume erosion were observed. The initial structure of the studied biodegradable fibres had a strong effect on the degradation, which was shown by photographic documentation and analysis of mass loss kinetics. The onset time for the amorphous material with high molar mass and D-lactide content was less than 1 day, while for the semicrystalline material it was nearly 2 days. The erosion profiles and pseudo-first-order rate of erosion constant were also variable and dependent on the initial structure. It is worth noting that the experiment demonstrated the lack of influence or insignificant influence of the pH of the applied degradation medium on the process kinetics. This is due to an increase in temperature of the process to the value at the point where the pH is not affected by hydrolysis.

The molecular structure was also changed during thermal-supported hydrolytic degradation, but in this case the influence of the initial structure on the process rate was less significant than in the macrostructure change. The calculated degradation time of half intrinsic viscosity for the amorphous samples with the highest molar mass was around 1 day, while for semicrystalline material with the

lower molar mass it was around 1.5 days. Based on the obtained results, it is supposed that the initial supramolecular structure has an effect on the degradation rate at the molecular level.

To summarize the experiment, it should be stated that the initial structure and supramolecular ordering had the greatest influence on the macroscopic effects of the degradation, and for the adopted degradation temperature of 90 °C, the influence of the pH of the degradation medium on the degradation kinetics was marginal.

Acknowledgments: The presented research was performed within the framework of a key project entitled "Biodegradable fibrous products" (Biogratex), which was supported by the European Regional Development Fund, Agreement No. POIG.01.03.01-00-007/08-00 and part of work was funded by statutory research fund of the Institute of Material Science of Textiles and Polymer Composites no. I-42/501/4-42-1-1

Author Contributions: M.G. conceptualization, data curation, formal analysis, investigations, visualization, writing – original draft; M.P. supervision, formal analysis; writing – original draft; G.S. investigations, visualization; I.K. writing – review & editing, funding acquisition.

References

1. Groot, W.; van Krieken, J.; Sliekersl, O.; de Vos, S. Production and Purification of Lactic Acid and Lactide In Poly(lactic acid): Synthesis, Structures, Properties, Processing, and Applications; Auras, R.; Lim, L-T.; Selke, S.E.M.; Tsuji, H., Eds.; John Wiley & Sons Inc., Hoboken, USA, 2010, pp. 3-19, ISBN: 978-0-470-29366-9.
2. Middleton, JC.; Tipton, AJ.; Synthetic biodegradable polymers as orthopedic devices. *Biomaterials* 2000, *21(23)*, 2335-2346, DOI: 10.1016/s0142-9612(00)00101-0.
3. Kale, G.; Auras, R.; Singh, SP. Degradation of Commercial Biodegradable Packages under Real Composting and Ambient Exposure Conditions. *Journal of Polymers and the Environment* 2006, *14(3)*, 317-334, DOI: 10.1007/s10924-006-0015-6.
4. Luo, Y.; Zhang, J.; Qi, R,; Hu, X., Pingkai, J. Polylactide Foams Prepared by a Traditional Chemical Compression-Molding Method. *Journal of Applied Polymer Science* 2013, DOI: 10.1002/app.39023.
5. Standau, T.; Chunjing, Z.; Castellón, S.M.; Bonten, Ch.; Alstadt, V. Chemical Modification and Foam Processing of Polylactide (PLA), *Polymers* 2019, *11(2)*, 306, DOI: 10.3390/polym11020306.
6. Tsai, Ch.; Wu, R.; Cheng, H.; Li, S.; Siao, Y.; Kong, D.; Jang, G. Crystallinity and dimensional stability of biaxial oriented poly(lactic acid) films, *Polymer Degradation and Stability*, 2010, *95(8)*, 1292-1298, DOI: 10.1016/j.polymdegradstab.2010.02.032.
7. Manich, AM.; Miguel, R.; Lucas, J.; Franco, F.; Baena, B.; Carilla, J.; Montero, L.; Cayuela, D. Texturing, stretching and relaxation behaviour of polylactide multifilament yarns, *Textile Research Journal* 2011, *81(17)*, 1788-1795, DOI: 10.1177/0040517511411972.
8. Solarski, S.; Ferreira, M.; Devaux, E. Characterization of the thermal properties of PLA fibers by modulated differential scanning calorimetry, *Polymer* 2005, *46(25)*, 11187-11192, DOI: 10.1016/j.polymer.2005.10.027.
9. Liu, Y.; Cheng, B.; Cheng, G. Development and Filtration Performance of Polylactic Acid Meltblowns, *Textile Research Journal* 2010, *79(16)*, 771-779, DOI: 10.1177/0040517509348332.
10. Puchalski, M.; Sulak, K.; Chrzanowski, M.; Sztajnowski, S.; Krucińska, I. Effect of processing variables on the thermal and physical properties of poly(L-lactide) spunbond fabrics, *Textile Tesearch Journal* 2015, *85(5)*, 535-547, DOI: 10.1177/0040517514547215.
11. Krucińska, I.; Surma, B.; Chrzanowski, M.; Skrzetuska, E.; Puchalski, M. Application of melt-blown technology in the manufacturing of a solvent vapor-sensitive, non-woven fabric composed of poly(lactic acid) loaded with multi-walled carbon nanotubes, *Textile Research Journal* 2013, *83(5)*, 859-870, DOI: 10.1177/0040517512460293.
12. Papageorgiou ,G.; Beslikas, T.; Gigis, J.; Christoforides, J.; Bikiaris, D. Crystallization and Enzymatic Hydrolysis of PLA Grade for Orthopedics, *Advances in Polymer Technology* 2010, *29(4)*, 280–299, DOI: 10.1002/adv.20194.
13. Wang, H.; Wei, Q.; Wang, X.; Gao, W.; Zhao, W. Antibacterial Properties of PLA Nonwoven Medical Dressings Coated with Nanostructured Silver, *Fibers and Polymers* 2008, *9(5)*, 556-560, DOI: 10.1007/s12221-008-0089-y.

14. Dharmalingam, S.; Hayes, D.; Wadsworth, L.; Dunlap, R. Analysis of the time course of degradation for fully biobased nonwoven agricultural mulches in compost-enriched soil, *Textile Research Journal* 2016, *86(13)*, 1343–1355, DOI: 10.1177/0040517515612358.
15. Czekalski, J.; Krucińska, I.; Kowalska, S.; Puchalski, M. Effect of Twist Stabilisation and Dyeing on the Structural and Physical Properties of Agricultural Strings, *Fibres and Textiles in Eastern Europe* 2013, *6(102)*, 39-44,
16. Tsuji, H. Polylactides. In Biopolymers. Polyesters III - Applications and Commercial Products; Doi, Y., Steinbüchel, A., Eds.; Weinheim: Wiley-VCH Verlag GmbH, 2002, pp. 129-177, ISBN: 978-3-527-30225-3
17. Henton DE, Gruber P, Lunt J and Randall J Polylactic acid technology. In Natural fibers, biopolymers, and biocomposites; Mohanty A.K. and Misra M., Eds.; Boca Raton: CPC Press, 2005, pp. 527-577.
18. Saeidlou, S.; Huneault, M.A.; Li, H.; Park, C.B. Poly(lactic acid) crystallization, *Progress in Polymer Science* 2012, *37(12)*, 1657-1677. DOI: 10.1016/j.progpolymsci.2012.07.005.
19. Saha, S.K.; Tsuji, H. Effects of molecular weight and small amounts of D-lactide units on hydrolytic degradation of poly(L-lactic acid)s, *Polymer Degradation and Stability* 2006, *91(8)*, 1665-1673, DOI: 10.1016/j.polymdegradstab.2005.12.009.
20. Zhang, N.; Yu, X.; Duan, J.; Yang, J.; Huang, T.; Qi, X.; Wang, Y. Comparison study of hydrolytic degradation behaviors between α'- and α-poly(L-lactide), *Polymer Degradation and Stability* 2018, *148*, 1–9, DOI: 10.1016/j.polymdegradstab.2017.12.014.
21. Fukushima, K.; Tabuani, D.; Dottori, M.; Armentano, I.; Kenny, J. M.; Camino, G.; Effect of temperature and nanoparticle type on hydrolytic degradation of poly(lactic acid) nanocomposites, *Polymer Degradation and Stability* 2011, *96(12)*, 2120-2129, DOI: 10.1016/j.polymdegradstab.2011.09.018.
22. Duan, J.; Xie, Y.; Yang, J.; Huang, T.; Zhang, N.; Wang, Y.; Zhang, J. Graphene oxide induced hydrolytic degradation behavior changes of poly(L-lactide) in different mediums, *Polymer Testing* 2016, *56*, 220-228, DOI: 10.1016/j.polymertesting.2016.10.015.
23. Chen, H.; Shen, Y.; Yang, J.; Huang, T.; Zhang, N.; Wang, Y.; Zhou, Z. Molecular ordering and α'-form formation of poly(L-lactide) during the hydrolytic degradation, *Polymer* 2013, *54(24)*, 6644-6653, DOI: 10.1016/j.polymer.2013.09.059.
24. Simmons, H.; Kontopoulou, M. Hydrolytic degradation of branched PLA produced by reactive extrusion, *Polymer Degradation and Stability* 2018, *158*, 228-237, DOI: 10.1016/j.polymdegradstab.2018.11.006.
25. Xu, L.; Crawford, K.; Gorman, Ch. Effects of Temperature and pH on the Degradation of Poly(lactic acid) Brushes, *Macromolecules* 2011, *44(12)*, 4777–4782, DOI: 10.1021/ma2000948.
26. Andrzejewska, A. One Year Evaluation of Material Properties Changes of Polylactide Parts in Various Hydrolytic Degradation Conditions, *Polymers* 2019, *11(9)*, 1496, DOI: 10.3390/polym11091496.
27. Cuadri, A.A.; Martín-Alfonso, J.E. Thermal, thermo-oxidative and thermomechanical degradation of PLA: A comparative study based on rheological, chemical and thermal properties, *Polymer Degradation and Stability* 2018, *150*, 37–45, DOI: 10.1016/j.polymdegradstab.2018.02.011.
28. Ricardo Acioli-Moura, Xiuzhi Susan Sun, Thermal Degradation and Physical Aging of Poly(lactic acid) and its Blends With Starch, *Polymer Engineering and Science* 2008, *48(4)*, 829-836, DOI: 10.1002/pen.21019.
29. Chávez-Montes, W.M.; González, G.; López-Martínez, E.I.; de Lira-Gómez, P.; de Lourdes Ballinas, E.; Flores-Gallardo, S. Effect of Artificial Weathering on PLA/Nanocomposite Molecular Weight Distribution, *Polymers* 2015, 7(4), 760-776, DOI: 10.3390/polym7040760.
30. Sztajnowski, S.; Krucińska, I.; Sulak, K.; Puchalski, M.; Wrzosek, H.; Bilska, J. Effects of the Artificial Weathering of Biodegradable Spun-Bonded PLA Nonwovens in Respect to their Application in Agriculture, *Fibres and Textiles in Eastern Europe* 2012, *96(6)*, 89-95
31. Zhang, H.; McGill, E.; Ohep Gomez, C.; Carson, S.; Neufeld, K.; Hawthotne, I.; Smukler, S. Disintegration of compostable foodware and packaging and its effect on microbial activity and community composition in municipal composting, *International Biodeterioration & Biodegradation* 2017, *125*, 157-165, DOI: 10.1016/j.ibiod.2017.09.011.
32. Gutowska, A.; Jóźwicka, J.; Sobczak, S.; Tomaszewski, W.; Sulak, K.; Miros, P.; Owczarek, M.; Szalczyńska, M.; Ciechańska, D.;Krucińska, I. In-Compost Biodegradation of PLA Nonwovens, *Fibres and Textiles in Eastern Europe* 2014; *22(5)*, 99-106.
33. Rudnik, E.; Briassoulis, D. Degradation behaviour of poly(lactic acid) films and fibres in soil under Mediterranean field conditions and laboratory simulations testing, *Industrial Crops and Products* 2011, *33(3)*, 648–658, DOI: 10.1016/j.indcrop.2010.12.031.

34. Puchalski, M.; Siwek, P.; Panayotov, N.; Berova, M.; Kowalska, S.; Krucińska, I. Influence of Various Climatic Conditions on the Structural Changes of Semicrystalline PLA Spun-Bonded Mulching Nonwovens during Outdoor Composting, *Polymers* 2019, *11(3)*, 559, DOI: 10.3390/polym11030559.
35. Sikorska, W.; Richert, J.; Rydz, J.; Musiol, M.; Adamus, G.; Janeczek, H.; Kowalczuk, M. Degradability studies of poly(L-lactide) after multi-reprocessing experiments in extruder, *Polymer Degradation and Stability* 2012, *97(10)*, 1891-1897, DOI: 10.1016/j.polymdegradstab.2012.03.049.
36. Puchalski, M.; Kwolek, S.; Szparaga, G.; Chrzanowski, M.; Krucińska, I. Investigation of the Influence of PLA Molecular Structure on the Crystalline Forms (α' and α) and Mechanical Properties of Wet Spinning Fibres, *Polymers* 2017, *9(1)*, 18, DOI: 10.3390/polym9010018.
37. Mao, Y.; Wei, W.; Zhang, J.; Li, Y. A novel determination technique of polymer viscosity-average molecular weights with flow piezoelectric quartz crystal viscosity sensing, *Journal of Applied Polymer Science* 2001, *82(1)*, 63-69, DOI: 10.1002/app.1823.
38. Behera, K.; Chang, Y-H.; Chiu, F-Ch.; Yang, J-Ch. Characterization of poly(lactic acid)s with reduced molecular weight fabricated through an autoclave process, Polymer Testing 2017, 60, 132-139, DOI: 10.1016/j.polymertesting.2017.03.015.
39. Puchalski, M.; Krucińska, I.; Sulak, K.; Chrzanowski, M.; Wrzosek, H. Influence of the calender temperature on the crystallization behaviors of PLA spun bonded non-woven fabrics, *Textile Research Journal* 2013, *83(17)*, 1775-1785, DOI: 10.1177/0040517513478480.
40. Rabiej, M. Application of immune and genetic algorithms to the identification of a polymer based on its X-ray diffraction curve, *Journal of Applied Crystallography* 2013, *46(4)*, 1136-1144, DOI: 10.1107/S0021889813015987.
41. Azimi, B.; Nourpanah, P.; Rabiee, M.; Arbab, S. Poly (lactide -co- glycolide) Fiber: An Overview, *Journal of Engineered Fibers and Fabrics* 2014, *9*, 47-66, DOI:10.1177/155892501400900107.
42. Kenley, R.A.; Lee, M.O.; Mahoney, T.R.; Sanders, L.M. Poly(lactide-co-glycolide) Decomposition Kinetics in Vivo and in Vitro, *Macromolecules* 1987, *20*, 2398-2403, DOI:10.1021/ma00176a012.
43. Ho, K-L.G.; Pometto III, A.L.; Gadea-Rivas, A.; Briceno, J.A.; Rojas, A. Degradation of Polylactic Acid (PLA) Plastic in Costa Rican Soil and Iowa State University Compost Rows, *Journal of Environmental Polymer Degradation* 1999, *7(4)*, 173-177, DOI:10.1023/A:1022874530586.
44. Pitt, G.G.; Gratzl, M.M.; Kimmel, G.L.; Surles, J.; Schindler A., Aliphatic polyesters II. The degradation of poly(DL-lactide), poly(ε-caprolactone), and their copolymers in vivo, *Biomaterials* 1981, l2, 215-220, DOI: 10.1016/0142-9612(81)90060-0.
45. Stoclet, G.; Seguela, R.; Vanmansart, C.; Rochas, C.; Lefebvre, J-M. WAXS study of the structural reorganization of semi-crystalline polylactide under tensile drawing, *Polymer* 2012, *53(2)*, 519-528, DOI: 10.1016/j.polymer.2011.11.063.
46. Avrami, M. Kinetics of Phase Change. II Transformation-Time Relations for Random Distribution of Nuclei, *Journal of Chemical Physics* 1940, *8*, 212, DOI: 10.1063/1.1750631.
47. Jeziorny, A. Parameters characterizing the kinetics of the non-isothermal crystallization of poly(ethylene terephthalate) determined by d.s.c., *Polymer* 1978, *19(10)*, 1142-1144, DOI: 10.1016/0032-3861(78)90060-5.